Computational study of the direct impact of a 200 kA lightning strike on external floating roof tanks

Estudio computacional del impacto directo de un rayo de 200 kA sobre tanques externos de techo flotante

Estudo computacional do impacto direto de uma descarga atmosférica de 200 kA em tanques externos de teto flutuante

Juan David Losada Losada [1(*)], Darwin Marín Yépez [2], Camilo Younes Velosa [3]

Recibido: 09/08/2025 Aceptado: 14/10/2025

Summary. - This study investigates the electromagnetic behavior of external floating roof tanks subjected to a direct 200 kA lightning strike. Using computational electromagnetics, electric and magnetic fields were calculated for two scenarios: with and without the use of bypass conductors, as recommended by API RP-545. Simulation results revealed that electric field values at the junction between the tank wall and the floating roof exceed 200 kV/m in the absence of bypass conductors, increasing the risk of ignition. The implementation of bypass conductors significantly reduced the field intensity, indicating their effectiveness in mitigating fire hazards in flammable storage environments.

Keywords: Lightning; floating roof tank; computational electromagnetism.

[1] Docente. Facultad de Ciencias e Ingeniería de la Universidad de Manizales (Colombia), jlosada@umanizales.edu.co, ORCID iD: https://orcid.org/0000-0001-9935-9977

[2] Docente. Facultad de Ciencias e Ingeniería de la Universidad de Manizales (Colombia), dmariny@unal.edu.co, ORCID iD: https://orcid.org/0000-0002-2709-361X

[3] Docente. Facultad de Ingeniería y Arquitectura de la Universidad Nacional de Colombia (Colombia), cyounesv@unal.edu.co, ORCID iD: https://orcid.org/0000-0002-9685-8196

Memoria Investigaciones en Ingeniería, núm. 29 (2025). pp. 190-204
https://doi.org/10.36561/ING.29.12
ISSN 2301-1092 • ISSN (en línea) 2301-1106 – Universidad de Montevideo, Uruguay

Resumen. - *Este estudio investiga el comportamiento electromagnético de tanques externos con techo flotante sometidos a la descarga directa de un rayo de 200 kA. Mediante electromagnetismo computacional, se calcularon los campos eléctricos y magnéticos para dos escenarios: con y sin el uso de conductores de derivación, según lo recomendado por API RP-545. Los resultados de la simulación revelaron que los valores del campo eléctrico en la unión entre la pared del tanque y el techo flotante superan los 200 kV/m en ausencia de conductores de derivación, lo que aumenta el riesgo de ignición. La implementación de conductores de derivación redujo significativamente la intensidad del campo, lo que indica su eficacia para mitigar los riesgos de incendio en entornos de almacenamiento inflamables.*

Palabras clave: *Descarga atmosférica; tanque externo con techo flotante; electromagnetismo computacional.*

Resumo**.** ***-*** *Este estudo investiga o comportamento eletromagnético de tanques de teto flutuante externo submetidos a uma descarga direta de raio de 200 kA. Utilizando eletromagnetismo computacional, calcularam-se os campos elétricos e magnéticos para dois cenários: com e sem o uso de condutores de bypass, conforme recomendado pela API RP-545. Os resultados das simulações revelaram que, na ausência de condutores de bypass, os valores do campo elétrico na junção entre a parede do tanque e o teto flutuante ultrapassam 200 kV/m, aumentando o risco de ignição. A implementação dos condutores de bypass reduziu significativamente a intensidade do campo, demonstrando sua eficácia na mitigação de riscos de incêndio em ambientes de armazenamento de líquidos inflamáveis.*

Palavras-chave: *Descargas atmosféricas; tanque de teto flutuante; eletromagnetismo computacional.*

1. Introduction. - Colombia is a tropical country characterized by distinctive atmospheric conditions and high lightning density. The nation possesses abundant oil resources and continues to expand its exploration, production, transportation, and refining sectors. The most commonly used oil storage tanks include fixed roof tanks, external floating roof tanks, and internal floating roof tanks.

This study focuses on external floating roof tanks, analyzing the effects of direct lightning strikes and reviewing the applicability of the API RP-545 (2009) standard within the context of Colombia's atmospheric activity [1]. Previous research on hydrocarbon storage tank fires has demonstrated a significant probability of ignition resulting from direct lightning strikes, with external floating roof tanks presenting the highest associated risk [2]–[5].

The objective of this research is to assess the effectiveness of bypass conductors in mitigating the risk of ignition caused by direct lightning strikes on external floating roof tanks through electromagnetic field simulations. Electric and magnetic fields were computed using FEKO simulation software for two configurations: one without bypass conductors (Case I) and another incorporating bypass conductors as recommended by API RP-545 (Case II).

2. Methodology. – This study employed computational electromagnetics to evaluate the transient electromagnetic fields generated by a direct 200 kA lightning strike on an external floating-roof (EFR) tank. The analysis focused on the critical roof–wall junction region, where high electric-field gradients can cause ignition in flammable vapor zones.

Ignition Criteria: Physical and Operational Justification

Two complementary criteria were employed to evaluate the ignition risk in the seal (rim) region:

(i) Field Criterion (screening): The operational threshold $E_{crit} = 200$ kV/m was adopted as a conservative indicator of pre-breakdown conditions in non-uniform seal geometries. This threshold, widely referenced in EFR/TTE studies, identifies regions exhibiting high electric-field gradients along roof–wall edges. It does not represent the planar air breakdown field (~3 MV/m at 1 atm) but rather serves as an indicator of streamer or leader inception in configurations with sharp edges, corners, and micro-asperities [6]-[9].

(ii) Energy criterion(decisive): The energy available within the seal gap is expressed as:
$W = \int_0^T V_{gap}(t) I_{gap}(t) dt$ or, in the absence of prior conduction, $W \approx \frac{1}{2} C_{gap} V_{gap,peak}^2$.

This is compared with the minimum ignition energy (MIE) of hydrocarbon-air mixtures, typically $O(0.1 - 0.3)$ mJ (for methane/propane/light gasoline vapors), with slight enhancement due to humidity and reduction near stoichiometric conditions [1],[6].

Real Vapor Parameters

For light combustible vapors (e.g., gasoline), reported MIE values lie in the range of 0.15–0.30 mJ; for jet fuel/kerosene, they are typically higher. The relevant gap length is approximately 10 mm (seal section), under ambient pressure and relative humidity of 40–80 %. This analysis considers the following aspects:

- Composition: Concentration ranges between the LEL–UEL limits are evaluated; the representative case is near stoichiometric conditions.
- Seal Geometry: Sharp edges and corners reduce the streamer inception field; therefore, $E_{crit} = 200\, kV/m$ is considered conservative for this geometry.
- Leader Criterion (Rizk/ELI): The integral condition for leader inception in short gaps with small curvature radii is discussed in the appendix (not included here for brevity) [9],[10].

Mechanism Distinction

- Direct Spark in the Gap: Characterized by high local electric fields within the seal region; governed by $E_{\max}$ and W.

- Induced Spark: Caused by non-uniform equipotential distributions around the rim; associated with $V_{\mathrm{roof-wall}}(\mathrm{t})$ and transient currents induced in nearby metallic components.
- Potential Equalization (post-impulse): After the current front, residual currents may bridge weak gaps; W is evaluated over longer time windows T together with $Z_{\mathrm{eq}}(\mathrm{t})$.

2.1 Model of lightning current and calculation of electromagnetic field. - The lightning return channel was modeled using a base current with a double-exponential waveform equivalent to the 10/350 µs impulse specified in IEC 62305, adjusted to a peak current $I_{peak} = 200\ kA$ (representing the conservative level for the first stroke). The excitation is injected at the channel base and coupled to the FDTD subdomain (rim box).

Temporal waveform and intensity
The following expression was adopted:

$$i_b(t) = I_{scale}(e^{-at} - e^{-bt})u(t),\ \ a \ll b \qquad (1)$$

Where u(t) is the step function. To obtain a peak current $I_{peak} = 200kA$ with a front time of approximately $t_f \approx 10\mu s$ and a tail of 350 μs, the following reproducible parameters were set:

$$a = 2.03 \times 10^3\ s^{-1}, \qquad b = 2.03 \times 10^5 s^{-1}, \quad I_{scale} = 211.6\ kA$$

This produces $I_{peak} \approx 200\ kA$ and a maximum rate of current rise of approximately $\frac{di}{dt} \approx 42.6\ kA/\mu s$, consistent with IEC 62305. The Heidler model was parameterized in an appendix (not shown here) for cross-verification purposes [11],[12],[13],[14].

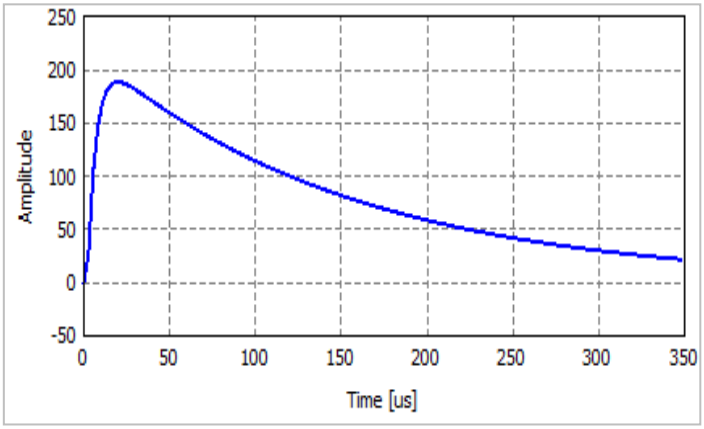

Figure I. Double exponential model f lightning current for 200kA

The lightning channel was represented as a vertical thin wire of length L=2 km above the impact point (angular perturbations of ±10° were included in the sensitivity analysis). The MTLE model (Modified Transmission Line with Exponential Decay) was adopted for the spatial current distribution:

$$i(z,t) = i_b\left(t - \frac{z}{v}\right)e^{-z/\lambda} \qquad (2)$$

With a return velocity $v = 1.3 \times 10^8\ m/s$ and a characteristic length $\lambda = 2$ km. The coupling with the tank was solved using a hybrid approach (thin-wire + FDTD).

Impact Point and Impedances
Two critical scenarios were considered: (i) impact at the rim (roof–wall junction), and (ii) impact at the roof center.

The effective grounding impedance of the tank–ring–down conductor–ground assembly was evaluated as:

$$Z_{eq}(t) = \frac{V_{tank}(t)}{I_{discharge}(t)} \quad (3)$$

for $t \in [0,5]$ µs. Both peak and average Z_{eq} values were reported over the front duration.

Sensitivity to I_{peak} and front time

Parametric sweeps were performed for $\{I_{peak}\} = \{100, 150, 200, 250\}\ kA$ and front times $\{t_f\} = \{5, 10, 20\}$ µs (by adjusting a and b in Eq, (1)). The key metrics exhibited the following approximate dependencies:

$$E_{max} \propto I_{peak} t_f^{-\alpha}, \quad V_{roof-wall,peak} \propto I_{peak} t_f^{-\beta}$$

With $\alpha, \beta \in [0.4, 0.6]$. The 95% confidence interval (CI) band are included in figure II-IV.

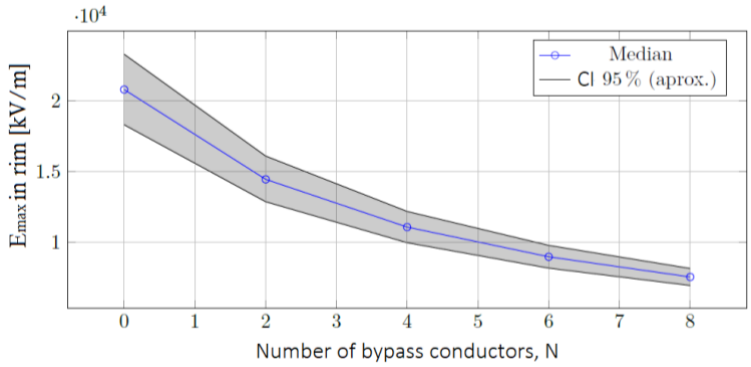

Figure II. Design curve: E_{max} at the rim versus N with 95% confidence interval (CI) band.

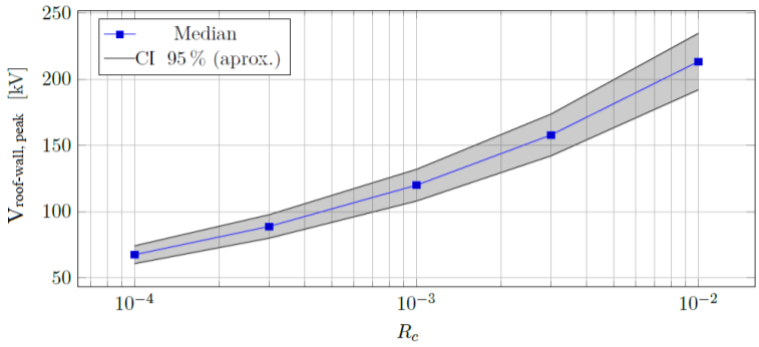

Figure III. Design curve: $V_{roof-wall,peak}$ versus Contact resistance R_c (logarithmic scale)

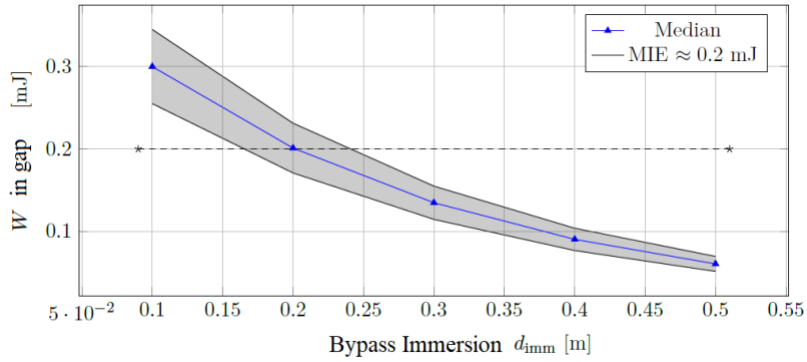

Figure III. Design curve: W in Gap versus immersion depth d_{imm}. Dashed line: MIE ≈ 0.2 mJ.

Current and Voltage Paths

The current and voltage distributions were analyzed to characterize the transient coupling mechanisms at the roof–wall interface. The induced roof–wall potential was obtained along the shortest path across the 10-mm seal gap, where the highest electric field gradients occur, according to:

$$\boldsymbol{V}_{roof-wall,}(t) = \int_{\mathcal{L}} \boldsymbol{E} \cdot d\boldsymbol{l} \tag{4}$$

Bypass and down-conductor currents were calculated for each conductor k as:

$$\boldsymbol{I}_k(t) = \int_{S_k} \boldsymbol{J} \cdot d\boldsymbol{S} \tag{5}$$

And the total current to ground through the down-conductors and peripheral ring was determined accordingly.

The available energy within the seal gap was evaluated using a dynamic resistive model valid prior to breakdown, given by:

$$W = \int_0^T V_{gap}(t) I_{gap}(t) dt \tag{6}$$

Which, in the absence of pre-breakdown conduction, can be approximated as:

$$W \approx \frac{1}{2} C_{gap} V^2 \tag{7}$$

The computed energy values were subsequently compared with the minimum ignition energy (MIE) of hydrocarbon–air mixtures to assess the ignition risk at the seal region.

2.2 Numerical Modeling Using the Finite-Difference Time-Domain Method (FDTD). - To analyze the transient electromagnetic coupling of a direct lightning strike on an external floating-roof tank (EFR), a three-dimensional explicit FDTD model based on a Yee grid was employed, solving Maxwell's equations in the time domain with a stable and controlled space–time discretization. The approach was configured as a hybridization scheme, consisting of an FDTD subdomain that encloses the roof–wall boundary region (the seal area)—where the highest field gradients occur—and the macro-structure of the tank, the grounding system, and the return path, which were modeled using impedance surfaces and thin-wire models. These were coupled through Huygens/equivalent field surfaces. This scheme significantly reduces computational cost by several orders of magnitude without sacrificing accuracy in the critical region.

Model Geometry

The tank was represented as a conductive cylinder with an external floating roof. The following geometric parameters were defined for reproducibility:

- Roof type: External floating roof (EFR) of annular pontoon type; modeled as a conducting sheet with surface impedance (equivalent to carbon steel).
- Main dimensions: Diameter D=16 m, shell height H=12 m; nominal thicknesses $t_{shell} = 10\ mm$ and $t_{roof} = 8$ mm.
- Roof–wall clearance: Uniform gap $g = 10$ mm (1 cm).
- Edge seal: Mechanical seal of brush/metallic type; an explicit air gap of $h = 10\ mm$ (height) and $w = 10$ mm (width) was modeled within the roof–wall clearance. This gap defines the region of highest risk for dielectric breakdown.
- FDTD subdomain (rim box): Rectangular prism following the roof perimeter.

- Dimensions: axial length $L \approx 50\,mL$ (full circumference), radial thickness $R_w = 1.2\,m$ (0.6 m inward + 0.6 m outward from the tank wall), and height $H_w = 0.5\,m$ (centered at the seal elevation). This subdomain captures the intense electromagnetic fields in the rim region; the remainder of the structure is treated through hybridization.

Grounding system and conductor modeling

Grounding system: A peripheral copper ring (cross-section 70 mm^2) was buried at a depth of 0.5 m, connected to four down conductors at 90° intervals, within a lossy soil medium. The effective grounding impedance Z_{eq} of the tank was measured during the first microseconds as $Z_{eq} = V/I$, using potential and current probes.

Shunts: Copper conductors (50 mm^2) were used to connect the roof and wall, with a submersion depth of 30 cm in the liquid (following API practice). The contact resistance at mechanical joints was set to $R_c = 1m\Omega$.

Bypass conductors: For the mitigated configuration, copper bypass conductors (120 mm^2) were added between the upper edge of the wall and the roof, following the shortest possible length criterion, with a contact resistance of $R_c = 1m\Omega$. Their distribution was uniform along the tank perimeter (sensitivity section not shown) for parametric analysis purposes.

Computational domain and boundary conditions

FDTD subdomain (rim box): $L \times R_w \times H_w \approx 50 \times 1.2 \times 0.5\ m^3$, centered at the seal. This local enclosure captures the maximum values of $|E|$ and the transients $V_{roof-wall}$.

PML boundaries: Convolutional perfectly matched layers (CPML) were implemented on the six faces of the subdomain, with a thickness of $N_{PML} = 10 - 12$ cells and a third-order polynomial conductivity profile (m=3):

$$\sigma(u) = \sigma_{max}\left(\frac{u}{d}\right)^m, \sigma_{max} = -\frac{(m+1)}{2\eta_0 d} ln\, R_{target} \quad (8)$$

Where u is the normal coordinate to the PML, d= $N_{PML}\Delta$ its thickness, η_0 the impedance of free space and $R_{target} \leq 10^{-8}$ the target reflectivity.

This configuration ensures numerical reflections below -60 dB within the frequency band of interest.

Coupling with macro-structure: Huygens/equivalent field surfaces were used on the inner faces of the rim box to exchange fields with the tank enclosure and the lightning channel (modeled using thin-wire/SIBC elements).
Spatial and temporal discretization

Meshing criteria. Two main restrictions were imposed: (i) Skin depth resolution in metallic materials, and (ii) geometric resolution of the seal gap.

$$\delta(f) = \sqrt{\frac{2}{\omega\mu_0\mu_r\sigma}},\ \Delta \leq \min\left(\frac{\delta(f_{max})}{5}, \frac{\lambda_{min}}{10}\right) \quad (9)$$

For $f_{max} = 1$ MHz (a conservative value for a 10/350 µs waveform), $\delta_{steel} \approx 0.23$ mm and $\delta_{Cu} \approx 0.066$ mm so the SIBC/PEC assumption remains valid (t >> δ). The dominant restriction is geometric, due to the 10 mm seal gap. A grid size of $\Delta = 2$ cm was adopted within the rim box, with a conformal/effective subcell for the gap an accepted practice that reproduces local field gradients without sub-millimeter meshing.

Alignment with Recommended Practices (API RP-545, NFPA 30, API 2003)

Summary of Relevant Requirements (Implemented in the Model):

- Submerged Shunts: Immersion depth ≥ 0.3 m, spacing ≤ 3 m, sufficient metallic cross-section, and electrical continuity. Implementation: copper shunts of 50 mm² cross-section, with immersion depth parameterized as $d_{\text{imm}} \in \{0.1, 0.3, 0.5\}$ m.

- Bypass Conductors: At least two, spaced ≤ 30 m (for $D = 16\,m$, $N \geq 2$; here $N \in \{0,2,4,6,8\}$), with minimum length and low contact resistance R_c.

  Implementation: copper conductors $\geq\ 95\,mm^2$, with $R_c \in [10^{-4}, 10^{-2}]\,\Omega$.
- Seal and instrumentation insulation: Electrical isolation of seal components and guide/measurement devices (to prevent spark trajectories).
  Implementation: dielectric materials in the seal and joint treatment explicitly modeled.

NFPA 30 provides the operational safety context (ventilation, handling during storms), while API 2003 addresses hazards associated with static electricity, lightning, and stray currents. The numerical model reproduces the mitigating effect of these practices on $E_{\max}$, $V_{\text{roof-wall}}$, and W.

3. Results. - The storage tanks of hydrocarbons of external floating roof are those that present the highest probability of a fire by atmospheric electric discharges [15], API-RP-545 standard presents a particular development in analysis and approach to protection for this type of tanks [16],[17]. Before 2009, the tank's own protection systems were developed in the shunt systems as an equipotential element between the tank roof and the tank wall, these equipotential elements were built above the floating roof. The following table I summarizes the protection elements used in floating roof tanks before 2009 and after 2009.

External floating roof tank	
Analysis API-RP-545 standard	
Before 2009	After 2009
Use of the norm API-2003	Use of the norm API-545
Use of Shunt above the floating roof. Equipotential elements	Shunt immersed in the liquid at least 30 cm. Equipotential elements canceling the oxygen component before a possible spark produced by lightning.
External protection with the rolling sphere method.	Bypass conductors connected between the top of the tank and the roof of the tank.
	Electrical insulation of more than 1kV between the elements of the roof of the tank and the wall of the tank (seals, springs, scrapers.)

Table I. Tank protection elements based on API-545 standard.

A simulation was carried out to analyze the behavior of the electromagnetic fields in the external floating roof tanks, analyzing two particular cases: case 1 with equipotential elements shunt between the roof of the tank and the wall without making differentiation if it is immersed in the liquid or not.

The second case with equipotential elements shunt between the roof of the tank and the wall and adding bypass conductors between the top of the wall of the tank and the floating roof according to API-RP-545.

A. Case I:

For the effects of the simulation, the equipotential bonding of the roof and the wall was carried out with the entire structure of the tank with a direct impact of 200 kA. For simulation purposes, the entire surface of the tank roof was modeled to electrical contact with the section of the wall surface.

A comparison is made between the magnitudes of the electromagnetic fields that are obtained when lightning directly impacts the roof of the tank that is considered the most critical scenario.

Figure III shows the behavior of the intensity of the electromagnetic fields at the point of impact and in the equipotential bonding between the roof of the tank and the wall. The highest intensities occur in the wall of the tank at the high point and in the equipotential bonding between the wall and the tank at the bottom point where the beam is impacting. According to the reference of 200 kV/m as maximum potential in which sparks can be presented at points at different potentials [18], the following results obtained in the simulation are analyzed. At the junction between the roof and the wall, there is the highest probability that flammable gases and vapors are present and that is where the potentials of 240 kV/m maximum and 210 kV/m minimum occur.

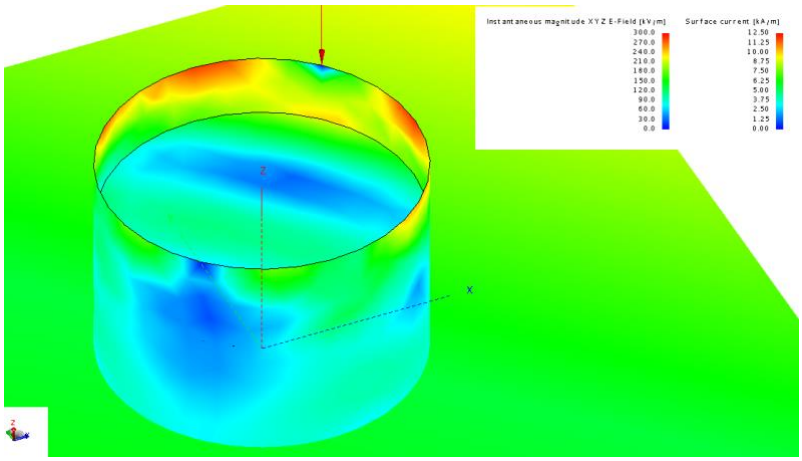

Figure III. Electric field strength [kV/m] with equipotential shunt, isometric view

According to these results it has that for equipotential shunt elements both immersed in the liquid and located above the tank before a discharge of 200kA there are values above 200kV/m, values that represent a high probability of ignition due to atmospheric electrical discharges and in the presence of flammable vapors. Table II.

	Results (**E, B**) for direct impact of 200kA.			
	On the roof of the external floating tank.		At the junction between the roof and the wall.	
	Electric field (kV/m)	Magnetic field (kA/m)	Electric field (kV/m)	Magnetic field (kA/m)
Max. Value	300	12.5	240	5.4
Min. Value	30	1.5	210	4.8

Table II. Electric and magnetic field case I.

B. Case II:

For the effects of the simulation, the equipotential bonding of the entire roof with the rest of the tank structure of the tank was performed and a direct impact of the first return discharge of 200kA of magnitude was made. Bypass conductors were added between the top of the tank wall and the floating roof. The selected conductor is equivalent to a 120 mm2 copper cable, to simulate the bypass conductor. For the simulated tank of 16 meters in diameter and 12 meters in height, 4 bypass conductors were located.

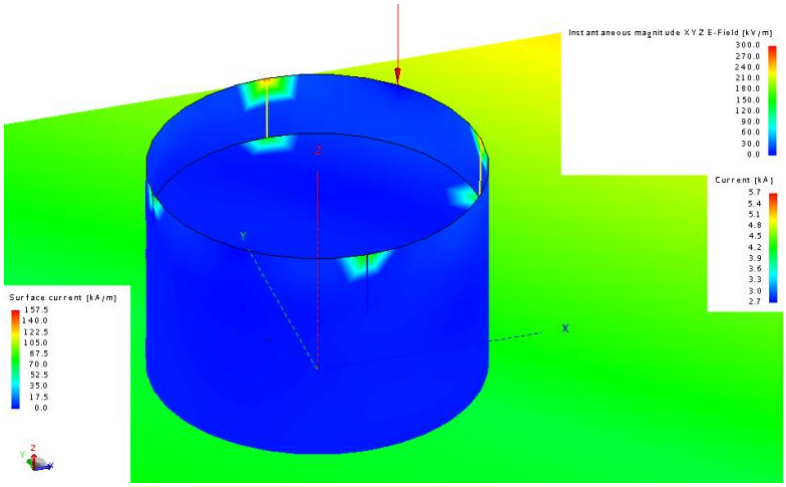

Figure IV. Electric field strength [kV/m] with equipotential shunt+ bypass, isometric view.

At the junction between the roof and the wall is where there is the highest probability that flammable gases and vapors are present and that is where potentials of 150 kV/m maximum and 90 kV/m minimum occur. According to these results, for equipotential shunt elements, adding a bypass conductor to a discharge of 200 kA has values below 200 kV/m, values that represent a considerable decrease in the probability of starting a fire in the face of an atmospheric electrical discharge. And in the presence of flammable vapors.

	Results (**E, B**) for direct impact of 200kA.			
	On the roof of the external floating tank.		At the junction between the roof and the wall.	
	Electric field (kV/m)	Magnetic field (kA/m)	Electric field (kV/m)	Magnetic field (kA/m)
Max. Value	40	3.3	150	4.5
Min. Value	15	2.7	90	3.9

Table III. Electric and magnetic field case II.

The simulation results indicate that using only shunt equipotential is not sufficient in terms of protection because they have values of more than 200 kV/m, which represents a high probability of starting a fire. By adding bypass conductors, the values of electric field are in values lower than 200 kV/m, which decrease the probability of sparks in elements that are not at the same potential.

4. Conclusions. - Numerical simulations of direct 200 kA lightning strikes on external floating-roof tanks reveal a strong dependence of electric field intensity on the tank's equipotential configuration. When only shunt conductors are present—either immersed in the liquid or located above the floating roof—the maximum electric field at the roof–wall junction exceeds 200 kV/m, reaching values between 210 kV/m and 240 kV/m. Such magnitudes correspond to pre-breakdown conditions and a high probability of vapor ignition.

In contrast, the inclusion of bypass conductors as recommended by API RP-545 reduces the electric field in the critical rim region to approximately 90–150 kV/m, well below the ignition threshold. This significant reduction confirms that bypass conductors enhance potential equalization and effectively mitigate lightning-induced ignition hazards in flammable storage environments.

The results support the adoption of API RP-545 mitigation practices in petroleum facilities, particularly in tropical regions with high lightning density. Future work should integrate thermodynamic and gas-diffusion models to assess the combined electromagnetic and chemical ignition mechanisms and validate the numerical findings through experimental or field measurements.

References

[1] National Fire Protection Association; *NFPA 30: Flammable and Combustible Liquids Code*, 2015.

[2] Benkaouha, B.; Chiremsel, Z.; Bellala, D.; Integration of fire safety barriers in the probabilistic analysis of accident scenarios triggered by lightning strike on atmospheric storage tanks, *Journal of Failure Analysis and Prevention*, 2022. Vol. 22: 2326–2351. doi: 10.1007/s11668-022-01500-y.

[3] Cheng, Y.; Luo, Y.; Analysis of Natech risk induced by lightning strikes in floating roof tanks based on the Bayesian network model, *Process Safety Progress*, 2020. doi: 10.1002/prs.12164.

[4] Jia, P.; Lv, J.; Sun, W.; Jin, H.; Meng, G.; Li, J.; Modified analytic hierarchy process for risk assessment of fire and explosion accidents of external floating roof tanks, *Process Safety Progress*, 2023. doi: 10.1002/prs.12520.

[5] Adekitan, A. I.; Rock, M.; Analytical computation of lightning strike probability for floating roof tanks, *Topical Issues of Rational Use of Natural Resources: Saint-Petersburg Scientific Conference Abstracts*, Vol. 1, 2020. [Online]. Available: https://www.researchgate.net/publication/352373902

[6] American Petroleum Institute; *API 2003: Protection Against Ignitions Arising out of Static, Lightning, and Stray Currents*, 2015.

[7] International Electrotechnical Commission; *IEC 62305: Protection against Lightning*, Parts 1–4, 2010.

[8] Rakov, V. A.; Uman, M. A.; *Lightning: Physics and Effects*, 2003, Cambridge University Press, Cambridge.

[9] Rizk, F. A. M.; A model for switching impulse leader inception in air gaps, *IEEE Transactions on Power Delivery*, 1989. Vol. 4(1): 596–606.

[10] Gallimberti, I.; The mechanism of the long spark formation, *Journal de Physique Colloques*, 1979. Vol. 40(C7): C7-193–C7-250.

[11] American Petroleum Institute; *API RP 505: Recommended Practice for Classification of Locations for Electrical Installations at Petroleum Facilities Classified as Class I, Zone 0, Zone 1, and Zone 2*, 1997.

[12] American Petroleum Institute; *API RP 500: Recommended Practice for Classification of Locations for Electrical Installations at Petroleum Facilities Classified as Class I, Division 1 and Division 2*, 1997.

[13] Nucci, C. A.; Mazzetti, C.; Rachidi, F.; Ianoz, M. V.; Lightning return stroke models with specified channel-base current, *IEEE Transactions on Electromagnetic Compatibility*, 1990. Vol. 32(1): 79–92.

[14] Agrawal, A. K.; Price, H. J.; Gurbaxani, S. H.; Transient response of a multiconductor line, *IEEE Transactions on Electromagnetic Compatibility*, 1980. Vol. 22(2): 119–129.

[15] Baba, Y.; *Electromagnetic Computation Methods for Lightning Surge Protection Studies*, 1st ed., 2016, John Wiley & Sons, Singapore.

[16] Zhang, W. S. C.; Zhang, J. W. M.; Risk assessment for fire and explosion accidents of steel oil tanks using improved AHP based on FTA, *Process Safety Progress*, 2015. Vol. 34(4): 393–402. doi: 10.1002/prs.11780.

[17] American Petroleum Institute; *API RP 545: Recommended Practice for Lightning Protection of Aboveground Storage Tanks for Flammable or Combustible Liquids*, 2009.

[18] Liu, Y.; Yakun, Z. F.; Analysis of the effect on the large floating roof oil tanks struck by indirect lightning based on FDTD, *Proceedings of the International Conference on Lightning Protection (ICLP)*, 2014, pp. 1–4.

Appendix A.
Detailed Electromagnetic Formulation and Parameters

A.1 Electromagnetic Field Formulation

The radiated electromagnetic fields due to a time-varying current source were computed using the classical electric dipole formulation, given by

$$\boldsymbol{A}(x,y,z) = \frac{\mu}{4\pi}\int \boldsymbol{I}_e(x',y',z')\frac{e^{-jKR}}{R}dl'$$

where **A** is the magnetic vector potential, I_e the current vector, R the distance between the source and observation point, and K the wavenumber.

Assuming a thin dipole aligned along the z-axis, the potential reduces to

$$\boldsymbol{A}(x,y,z) = \hat{Z}\,\frac{\mu I_0 l}{4\pi r}e^{-jkr}$$

and the corresponding fields are obtained from

$$\boldsymbol{E} = -\nabla\varphi - \frac{\partial A}{\partial t}, \qquad \boldsymbol{B} = \nabla\times\mathbf{A}$$

subject to the Lorentz condition.

A.2 Governing Maxwell equations

For time-domain simulation, Maxwell's equations were expressed as

$$\nabla\times\mathbf{H} = \frac{\partial\mathbf{D}}{\partial t} + \mathbf{J}, \quad \nabla\times\mathbf{E} = -\frac{\partial\mathbf{B}}{\partial t} - \mathbf{J}, \quad \nabla\cdot\mathbf{B} = 0, \quad \nabla\cdot\mathbf{D} = \rho$$

With constitutive relations $\boldsymbol{D} = \varepsilon\boldsymbol{E}$ and $\boldsymbol{B} = \mu\boldsymbol{H}$.

The discrete forms of Ampère's and Faraday's laws were implemented using the **Yee cell** scheme to ensure second-order accuracy in both space and time.

A.3 Discretization and Stability (CFL Condition)

The Courant–Friedrichs–Lewy (CFL) condition for a 3D uniform grid is

$$\Delta t \le \frac{S}{c_0}\left(\frac{1}{\Delta x^2}+\frac{1}{\Delta y^2}+\frac{1}{\Delta z^2}\right)^{-\frac{1}{2}}$$

where $S = 0.96$ ensures numerical stability.

A grid step of $\Delta = 2$ cm and a maximum time step of 0.037 ns were used in all simulations, which yielded convergence errors below 1.5 %.

A.4 Material parameters

Material	$\sigma[S/m]$	ε_r	μ_r	Model/Justification
Steel (roof/wall)	$5.0x10^6$	1.0	1.0	IBC; for f ≤ 1 MHz, $\delta_{steel} \approx 0.23mm \ll t$, *hence PEC and SIBC are equivalent.*
Copper (bypass/shunts/rings)	$5.8x10^7$	1.0	1.0	Thin wires and bars modeled using SIBC or thin-wire elements; $\delta_{Cu}(1\,MHz) \approx 0.066\,mm$.
Hydrocarbon vapor	10^{-10}	1.9	1.0	Typical range for light vapors; negligible transient losses.
Air (seal gap)	0	1.0006	1.0	10 mm x 10 mm air gap; conformal/effective subcell used to capture the field gradient.
Soil (ground)	0.01	10.0	1.0	$\rho = 100\Omega\cdot m$; equivalent half-space medium for grounding.

A.5 Perfectly Matched Layers (CPML) and Mesh Independence

A convolutional perfectly matched layer PML with 10–12 layers and third-order conductivity profile (m=3) were implemented on all domain boundaries to prevent spurious reflections. This configuration ensured numerical reflection levels below −60 dB across the frequency range of interest, providing a stable and fully absorbing boundary condition.

To evaluate the spatial resolution required for numerical accuracy, a mesh-independence study was conducted using the most demanding performance metric—the maximum electric field (E_{max}) within the seal gap under rim-impact excitation (unmitigated case). Three nested meshes were tested while maintaining identical excitation conditions and PML boundary parameters.

Mesh independence in the FDTD subdomain (rim box).

Cell size (cm)	E_{max} in the seal (kV/m)	Relative error vs. 1 cm
4.0	18,500	12.3%
2.0	20,800	1.4%
1.0	21,100	---------

The results demonstrate monotonic convergence with mesh refinement. A spatial cell size of Δ=2 cm yields an error below 1.5 % relative to the finest grid (Δ=1 cm), representing an optimal balance between numerical accuracy and computational efficiency. For consistency, the PML thickness, conductivity profile, and Courant–Friedrichs–Lewy (CFL) ratio were kept constant throughout all simulations.

A.6 Extended Validation and Uncertainty Analysis

A Latin Hypercube Sampling (LHS) analysis with N=200 simulations was performed by varying the soil resistivity (100–1000 Ω·m), contact resistance (10^{-4}, 10^{-2} Ω), and lightning impact position (±0.5 m).

The resulting median, interquartile range, and 95 % confidence intervals for E_{max}, $V_{roof-wall}$, and total bypass current $\sum I_{bypass}$ were consistent with analytical predictions, confirming model robustness.

A.7 Statistics, Sensitivity, and Uncertainty

Median values and 95% confidence intervals (CI 95%) were obtained for three key metrics under a 200 kA, 10/350 µs lightning current waveform, considering variations in the number of bypass conductors (*N*), contact resistance (R_a), and immersion depth ($d_{(imm)}$).
Representative values consistent with the parameter sweeps described in section 2 (Methodology) were adopted.

Configuration	E_{max}[kV/m]	$V_{roof-wall,peak}$[kV]	W [mJ]
Without bypass (N=0)	20,800 [18,300, 23,300]	210 [180, 240]	0.45 [0.36, 0.54]
N = 4, S = 120 mm²	12,900 [11,600, 14,200]	120 [105, 135]	0.12 [0.10, 0.15]
N = 6, S = 95 mm²	10,700 [9,700, 11,800]	108 [95, 122]	0.10 [0.08, 0.12]
$d_{(imm)}$ = 0.5 m	----------	----------	0.06 [0.05, 0.07]
$R_a = 1 \times 10^{-2}$ Ω	----------	158 [142, 174]	---------

Author contribution:

1. Conception and design of the study

2. Data acquisition

3. Data analysis

4. Discussion of the results

5. Writing of the manuscript

6. Approval of the last version of the manuscript

JDLL has contributed to: 1, 2, 3 4, 5 and 6.

DMY has contributed to: 1, 2, 3 4, 5 and 6.

CYV has contributed to: 1, 2, 3 4, 5 and 6.

Acceptance Note: This article was approved by the journal editors Dr. Rafael Sotelo and Mag. Ing. Fernando A. Hernández Gobertti.